Chapter 6

# Abstract Neuron Models

## § 1. The Need for and Nature of Abstract Neuron Models

Physiological models such as those looked at in the previous chapters are discovered and developed for the purpose of understanding the neuron. They are the fruit of scientific reduction aimed at explaining neuron behavior at a mechanistic level. However, the purpose of explaining neuron behavior is to lay the foundation for eventually explaining the behavior of the more complex biological structures found in the nervous system and, eventually, of the CNS itself. The next step up in the ladder of scientific knowledge from the neuron is the neural network.

It will not have escaped your attention that every additional mechanistic detail learned adds to the complexity of the neuron model. The Huguenard-McCormick model of thalamocortical relay neurons includes ten different ionotropic current components, not counting synaptic channels. Eight of these are described by differential equations. Then one has the differential equation for calcium buffering plus the membrane voltage differential equation, for a total of ten differential equations that must be solved per time step. In addition, the eight ionotropic current equations also have auxiliary variables ($m_\infty$ and $\tau$) that require the calculation one or two exponential equations (e.g. a Boltzmann function) during each time step. Thus, comprehending in detail the mechanisms that produce the observable phenomena for membrane potential comes at a cost of great increase in computational complexity. If one wishes to study a network of $n$ such neurons, the computational cost multiplies by a factor of at least order $n$ (plus, of course, the added cost of computing the synaptic channel equations).

It does not take very many neurons before the computational cost of doing the simulation becomes prohibitive. For example, Rulkov et al. [RULK1] have reported that simulating 2.5 seconds of "real time" data for a linear chain of 128 H-H-like neurons required 9.5 minutes of computer time on a fairly respectable high-performance computer. The H-H model they used was a reasonably efficient one previously reported by Mainen and Sejnowski [MAIN]. This was about 2000-fold more computing time than the result they obtained using their ***abstract neuron model***.

What is an abstract neuron model? In general, it is a model that produces the same input-output (I/O) behavior as a physiological neuron model but achieves this by replacing the mechanistic expressions of an H-H-like model with an alternate set of dynamical equations. These equations sacrifice representation of the neuron's internal details in favor of a more computationally efficient set of dynamical equations that aims only at reproducing the neuron's

I/O behavior with acceptable accuracy. To put this another way, it is a model focused on the signal processing *function* of the neuron rather than the physiological understanding of its *mechanisms*. Underlying its theoretical justification is the presupposition that in a neural network it is only the signal processing function of individual neurons, viewed as I/O relationships, that matters insofar as the behavior of the *network* is concerned. The need for abstract neuron models is practical (reduction of computational costs), but the validity of the approach is still laid to the idea that only "unnecessary" details are sacrificed in achieving the practical goal.

But how does one know when a detail is "unnecessary" and when a detail is "necessary"? The mere fact that one might not be interested in how many species of voltage-gated $K^+$ channels a neuron might have or what their individual ionotropic currents might do is not sufficient to make this an "unnecessary" detail. If accurate modeling of these currents is required in order for the I/O properties of the neuron to be accurate, then they are "necessary" details. "Unnecessary" and "necessary" refer not to where one's interests may lie; they refer to whether or not the detail is required to achieve the purposes of one's model.

This brings us to the consideration of what is often called the ***function vs. mechanism*** levels of system representation. In a loose sense, one can say that *function* is "what the system does" and *mechanism* is "how the system does it." The coalescence of a number of mechanisms in one system frequently results in a system function for which properties of the system come into being that are not identifiable in any one of its mechanisms. Such properties are called ***emergent properties*** and they are the consequence of ***interactions*** among the mechanisms. Grossberg tells us,

> The distinction between a network's emergent functional properties and its simple mechanistic laws also clarifies why the controversy surrounding the relationship of an intelligent system's abstract properties to its mechanical instantiation has been so enduring. Without a linkage to mechanism, a network's functional properties cannot be formally or physically explained. On the other hand, how do we decide which mechanisms are crucial for generating desirable functional properties and which mechanisms are adventitious? Two seemingly different models can be equivalent from a functional viewpoint if they both generate similar sets of emergent behaviors. An analysis which proves such a functional equivalence between models does not, however, minimize the importance of their mechanistic descriptions. Rather, such an analysis identifies mechanistic variations which are not likely to be differentiated by evolutionary pressures which select for these functional properties on the basis of behavioral success.
>
> Another side of such an evolutionary analysis concerns the identification of the fundamental network modules which are specialized by the evolutionary process for use in a variety of behavioral tasks. How do evolutionary variations of a single network module, or blueprint, generate behavioral properties which, on the level of raw experience, seem to be phenomenally different and even functionally unrelated? Although each specialized network may generate a characteristic bundle of emergent properties, parametric changes of these specialized networks within the framework of a single network may generate bundles of emergent properties that are qualitatively different. In order to identify the mechanistic unity behind this phenomenal diversity, appropriate analytic methods are again indispensable [GROSS10].

The second paragraph just quoted is particularly pertinent when we examine larger scale behaviors of networks. At the level of neuron modeling, what is immediately of concern to us is Grossberg's comment, "Two seemingly different models can be equivalent from a functional viewpoint if they both generate similar sets of emergent behaviors." In every abstract neuron model some or even *all* of its dynamical equations are completely different from those of the physiological description of the neuron. Furthermore, the abstract neuron will be described by fewer equations than the physiological neuron it is meant to *imitate*. Were this not so, there would be no point to having an abstract neuron model. How can two different models generate functional emergent properties similar enough to be called "the same"? The answer is found in the phenomenon of *interaction*.

One way to illustrate this concept is by an analogy. As you know, water is composed of hydrogen and oxygen and described by the chemical reaction $2H_2 + O_2 \rightarrow 2H_2O$ we all learned in high school chemistry. If one is designing a lawn sprinkler system or studying how best to design the hull of a ship, the particulars of hydrogen and oxygen are matters of practical indifference; only the properties of water, which are wholly different than either hydrogen or oxygen alone, matter. If one knew enough about water but had never heard of either hydrogen or oxygen, one could still design a ship or a lawn sprinkler.

So, too, it is in the case of abstract neuron models used in a neural network model. Imagine if you can that some set of mechanistic equations stands in the role of "hydrogen" and another set stands in the role of "oxygen" in our analogy. Now imagine the outcome of their interactions at the cell level as standing in the role of "water." If we adequately describe the properties of "water" by its own set of fewer equations, then from an input-output (functional) point of view, this second set of equations is ***sufficient*** for our purposes *provided these equations do not also predict behaviors that do not actually happen* at the network level or *fail to produce* functional consequences that *do* happen in the biological system.

Proper modeling at the level of the abstract neuron is thus a matter of proper choice of *level of description* and *description of the gross effects of mechanistic interactions*. In the language of the system theorist, the task of going from a lower-level mechanistic description to a higher-level functional description is called ***model order reduction***. If we view the hierarchy of levels of scientific descriptions as a ladder, descending to lower rungs on the ladder is scientific reduction; ascending to higher rungs on the ladder is model order reduction. A key task and responsibility of science is to accomplish both outcomes while at the same time providing the linkage between the rungs (the "rails of the ladder") so that our different descriptive rungs do not levitate in mid-air without a firm supporting structure.

Grossberg makes another remark which, although addressed at neural network modeling, is equally appropriate for abstract neuron modeling.

> A network model is usually easy to define using just a few equations. These equations specify the dynamical laws governing the model's nodes, or cells, including the processing *levels* in which these nodes are embedded. The equations also specify the *interactions* between these nodes, including which nodes are connected by pathways and the types of signals or other processes that go on in these pathways. Inputs to the network, outputs from the network, parameter choices within the network, and the initial values of network variables often complete the model description. Such components are common to essentially all real-time network models. Thus, to merely say that a model has such components is scientifically vacuous.
>
> How, then, can we decide when a network model is wrong? Such a task is deceptively simple. If the model's levels are incorrectly chosen, then it is wrong. If its interactions are incorrectly chosen, then it is wrong. And so on. The only escape from such a critique would be to demonstrate that a different set of levels and interactions can be correctly chosen, and shares similar functional properties with the original model. The new choice of levels and interactions would, however, constitute a new model. The old model would still be wrong. Such an analysis would show that the shared model properties are essentially model-independent, yet that there exist finer tests to distinguish between models [GROSS10].

Such is the intellectual framework and the scientific environment for model order reduction and for the development, evaluation, and employment of abstract neuron models. Here it is worth the reminder that the utility of all scientific models is *the ability to predict* phenomena. Merely because a model accurately reproduces some set of experimental test outcomes is no guarantee the model will correctly predict other functional I/O behaviors under conditions different from those of the experiment. Yet such predictions are the pragmatic justification for model development in science. Were this not so, any statistical curve fit to measured data would suffice for science, yet such curve fits are not means of understanding but rather means of description in advance of understanding. This is important for us to keep in mind as we look at the descriptions of the abstract neuron models that follow.

## § 2. The Wilson Models

The first abstract neuron model we will consider in detail is actually a class of model neurons, which we will call Wilson's models [WILS1]. Wilson's models are ***signal processing models***, thus abstract neuron models. The goal of these models, in Wilson's own words, is "to develop the simplest plausible approximation to neocortical neurons that is consistent with the observed diversity of dynamical behavior." Three features of Wilson's models are noteworthy here. First, the model neurons are approximate models of neocortical neurons, i.e. neuron types found in the neocortex (the thin outer layer of the mammalian brain commonly called "the gray matter"; the neocortex is thought to be the seat of "higher" cognitive, sensory, and motor functions). Second, Wilson's models maintain a fairly close coupling with the physiology of the neuron. They are

abstract neuron models, but the connection between them and their biological counterparts is very evident and easily understood. We will call this sort of model order reduction ***approximation*** modeling, in distinction from another kind of model order reduction we will call ***mimic*** modeling. Third, Wilson's models are classified according to ***signaling type*** rather than by the anatomical classifications of neocortical neurons, although there is fairly well-defined correspondence between signaling type and anatomical classification. Because the notion of classifying neurons by signaling type is pervasive in neural network theory, it is worthwhile for us to begin the discussion with an overview of neocortical neurons and their varieties in the neocortex.

## § 2.1 Neocortical Neurons

Anatomists describe the neocortex as being divisible into six distinct layers, numbered 1 to 6, and distinguished mainly by depth and the types of neurons found in each. Layer 1 is the outer-most layer (closest to the skull bones) and contains very few neurons. Layer 1 does contain many axons running relatively short distances and providing regional cortico-cortical interconnections. Layer 6 is the deepest layer, immediately adjacent to the brain's "white matter" – a volume of the brain containing billions of myelinated axons interconnecting more distant regions of the brain, including connections to subcortical brain structures. The first and most broad classification of neocortical neurons is the division between ***excitatory neurons*** (neurons for which signaling tends to excite action potentials in their postsynaptic target cells) and ***inhibitory neurons*** (neurons for which signaling tends to suppress action potential generation in their target cells). Excitatory neurons make up about 85% of all neurons in the neocortex, the remaining 15% being inhibitory interneurons.

Excitatory neurons are further divisible into two classes, pyramidal cells and spiny stellate cells. Pyramidal cells (PCs) are the projection neurons in the neocortex. They are so called because the cell body has a pyramidal shape. A long dendritic structure projects vertically from the cell body and spans many layers within the neocortex. PCs are found in layers 2 through 6. Their axons make local synaptic connections but also project via the white matter to other locations in the brain. PCs in layers 2 and 3 primarily make cortico-cortical projections to other locations in the neocortex and primarily target neurons located in these same layers. They also make projections to nearby regions via layer 1 and by short lateral projections in the other layers. PCs in layer 5 make lateral axonal projections over short distances in layer 6 and white-matter projections to the brain's basal ganglia. PCs in layer 6 also make short axonal projections via layer 6 and long white-matter projections to the thalamus (a subcortical structure in the brain). PCs account for about 65% of all the neurons in the neocortex.

Spiny stellate cells (SSCs) account for about 20% of all neurons in the neocortex. They are

interneurons located in layer 4, and they are one of the principal target cells for signals coming into the neocortex from the thalamus (the "central routing" structure for sensory information coming into the neocortex from the peripheral nervous system). Their output projections never leave the immediate vicinity of where the cell body is located, although they do make output projects up as far as layer 2. The word "stellate" means "star-shaped", a term that describes the shape of the cell. SSC dendrites are covered with tiny projections, called dendritic ***spines***, where the majority of excitatory synapses made to the cell are found. (Pyramidal cells also have a rich structure of dendritic spines). Within the broad classification of cells as PCs or SSCs one finds a rich variety of subspecies of cells.

The remaining 15% of all neocortical neurons are inhibitory interneurons (IINs). Although the IINs make up the smallest class of neocortical neurons insofar as sheer number of neurons is concerned, they also exhibit the richest variety of different species of neurons. The ten identified species of IINs are: (1) large basket cells (LBCs); (2) small basket cells (SBCs); (3) nested basket cells (NBCs); (4) bitufted cells (BTCs); (5) bipolar cells (BPCs); (6) double bouquet cells (DBCs)[1]; (7) neurogliaform cells (NGCs); (8) Martinotti cells (MCs); (9) chandelier cells (ChCs); and (10) Cajal-Retzius cells (CRCs). IINs are characterized by the absence of dendritic spines, and receive their excitatory synaptic inputs on their dendritic shafts. IINs are found in all layers of the neocortex, but different species of IINs do have different characteristic locations. This is summarized in Table I, the data for which is taken primarily from [TOLE].

## § 2.2 Signaling Types in Neocortical Neurons

A number of different taxonomy systems have been proposed over the years for classifying neurons on the basis of their signaling properties [BERT], [RINZ], [CONNb1-2]. The one used in Table I and largely adopted by Wilson is due to Connors et al. [CONNb1-2], [McCO2]. It recognizes four primary signaling type classifications: regular spiking (RS); fast spiking (FS); intrinsic bursting (IB); and continuous bursting (CB). These classifications are based on neurons' membrane responses to the injection of a supra-threshold test current under laboratory test conditions. Thus, the names do not describe normal *in vivo* behavior of these cells in response to biological excitation. The Connors-Gutnick-McCormick (CGM) system is probably the one in widest use, but there is no one official "standard taxonomy" system in use at this time.

Nature seems to have a way of upsetting even the most carefully wrought classification systems, and this is so for the CGM system and for others as well. Thus it is not uncommon to see

[1] At this time there is some evidence suggesting that an excitatory bipolar cell and an excitatory double bouquet cell might also exist. This is not yet confirmed.

**Table I: Brief Summary of Cortical Neuron Classes**

| Cell Type | Signaling Class | Primary Neurotransmitter | Co-localized Neuropeptide | Location of Cell Body | Dendritic Location | Principal Axonal Targets |
|---|---|---|---|---|---|---|
| PC | RS | glutamate | SOM, CCK | layers II-VI | all layers | WM, dendrites. |
| PC | IB | glutamate | | V | all layers | WM, dendrites. |
| SSC | RS | glutamate | | IV | IV | dendrites in II-IV. |
| LBC | FS, RS | GABA | NPY, CCK | III, V | | soma and proximal dendrites with sparse intra-laminar and intra-columnar projections and long inter-columnar projections. |
| SBC | FS, RS | GABA | VIP, CCK | III-V | | local soma and proximal dendrites with dense intra-laminar and intra-columnar projections. |
| NBC | FS, CB, RS | GABA | NPY, SOM CCK | III, V | | local soma and proximal dendrites with sparse to dense intra-laminar and intra-columnar projections. |
| BTC | FS, CB, RS | GABA | SOM, CCK, VIP | | | intra-columnar over all layers |
| BPC | FS, IS, CB, RS | GABA | VIP | II-IV | all layers | dendritic shafts over all layers but few and very restricted target cells. |
| e-BPC | ? | glutamate? | ? | II-IV | ? | dendrites. |
| DBC | FS, CB | GABA | VIP | II/III | ? | dendrites over all layers in a column. |
| e-DBC | ? | glutamate? | ? | II-V | ? | dendrites. |
| NGC | FS | GABA | | I, III/IV | local layer | dendritic shafts in the same layer, column. |
| MC | FS, CB, IS | GABA | NPY, SOM CCK NPY+SOM | VI | VI +? | dendrites with intra-laminar and intra-columnar projections and inter-columnar projections. |
| CRC | ? | GABA | | I | I | local dendrites. |
| ChC | FS, CB | GABA | | III, V | III, V/VI | local axons in same layer and column. |

PC=pyramidal cell; SSC=spiny stellate cell; LBC=large basket cell; SBC=small basket cell; NBC=nest basket cell; BTC=bitufted cell; BPC=bipolar cell; e-BPC=excitatory bipolar cell (putative); DBC=double bouquet cell; e-DBC=excitatory bitufted cell (putative); NGC=neurogliaform cell; MC=Martinotti cell; CRC=Cajal-Retzius cell; ChC=chandelier cell; RS=regular spiking; FS=fast spiking; CB=continuous bursting; IS=irregular spiking; GABA=gamma aminobutyric acid; NPY=neuropeptide Y; VIP=vasoactive intestinal peptide; SOM=somatostatin; CCK=cholecystokinine; WM=white matter.

enhancements and sub-categories appended to the primary distinctions (RS, FS, IB, CB), nor does this fourfold division fully take into account every neuron signaling response that has been discovered. In addition to these four, there are also "irregular spiking" responses (IS), "chattering" CB responses [GRAY1], "rhythmic firing" responses (RF), "low threshold spiking" responses (LTS), "stuttering cells" (STUT), and, no doubt, others that will turn up over time. Newer

taxonomies, e.g. [GUPT], are brought forth from time to time to help deal with fine shades of difference that are obscured in the older taxonomies such as the CGM classifications [TOLE].

An RS neuron injected with a supra-threshold test current initially fires at a relatively high rate (determined by the amount of injected current) but soon slows its firing rate and settles into a constant-frequency firing pattern. This behavior is called ***accommodation*** by some researchers and 'adaptation' by others. Its principal physiological mechanism is thought to be the slow activation of $Ca^{2+}$-dependent $K^+$ channels with contributions by the $K^+$ "M" current [McCO2] (see chapter 4). Many neurons contain high-voltage-gated $Ca^{2+}$ channels in their cell membranes. These VGCs normally cannot be opened by EPSPs due to synaptic inputs. However, when the cell fires an AP sufficient voltage is generated to open these VGCs. This results in an influx of $Ca^{2+}$ ions which bind to sites on the cytoplasmic side of the proteins that make up the $Ca^{2+}$-dependent $K^+$ channels, thereby opening these channels and hyperpolarizing the cell. The amount of resulting firing rate accommodation depends on the number and density of these channels and on the number and density of the high-voltage $Ca^{2+}$ VGCs. Most, but not all, pyramidal cells belong to the RS signaling type. Spiny stellate cells also belong to the RS-type class.

Figure 6.1 illustrates the RS-type firing response. The firing rate accommodation is clearly evident in the figure from examining the spacing between successive action potentials. The figure

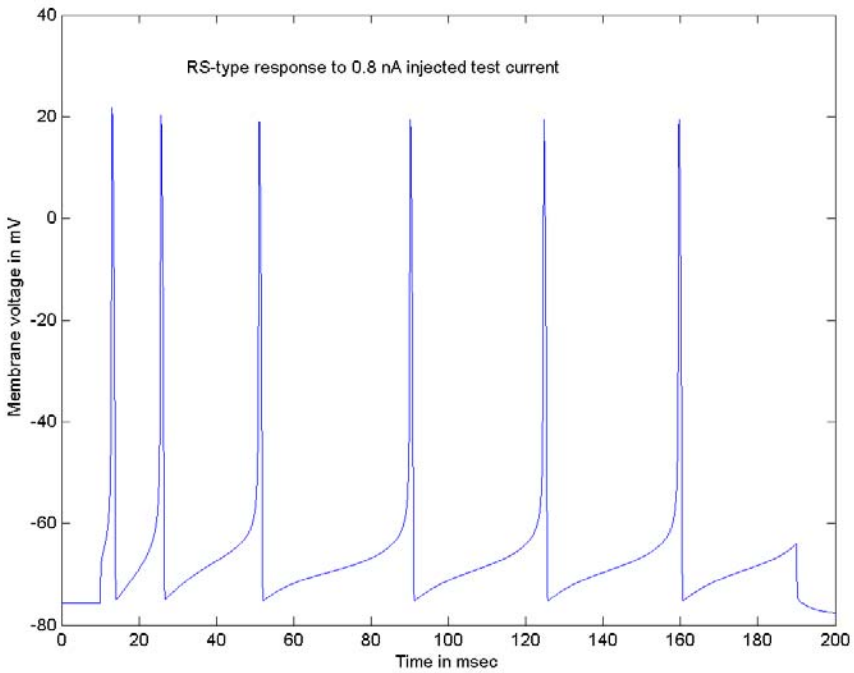


**Figure 6.1:** RS-type firing under laboratory test conditions stimulated by injection of an excitatory current from $t$ = 10 to $t$ = 190 ms.

was generated using Wilson's RS-type model parameters. In addition to the spike rate accommodation, one should also note the absence of any strong hyperpolarization during the repolarization of the membrane potential.

IB-type signaling is divisible into two major subclasses, called IB-1 and IB-2. Not all PCs are of the RS-type. Some PCs found in layer V exhibit IB-1 type signaling. The primary mechanism for IB-type firing is thought to be a transient low-threshold calcium current produced by low-voltage-gated $Ca^{2+}$ channels. It is this current, rather than an $Na^{+}$ current alone, that produces the burst action [McCO2]. However, the $Ca^{2+}$ channel is a slowly inactivating (transient) VGC and it soon ceases to conduct any more current until its inactivation is reset by hyperpolarizing the cell. Under laboratory test conditions with constant-current injection the neuron fires a burst of 3 to 5 action potentials, followed by a quite period, and then resumes firing at a lower and more or less constant rate. Other PCs exhibit IB-2 firing, where the neuron fires a burst, followed by a pause, then fires another burst, repeating this while the stimulus lasts. Figures 6.2 illustrate the IB-class responses.

The remaining 15% of neocortical neurons, the local inhibitory interneurons, are categorized into four classes. 50% of these neurons are classified as ***Class-I*** GABAergic cells. They are found in all cortical layers. Class-I IINs belong to the fast-spiking or FS-type category. As shown in Table I, almost all morphological classifications of IINs contain species of neurons belonging to Class-I. The classical FS-type neuron is non-accommodating, i.e. its spiking frequency does not change when the neuron is injected with an excitatory constant current. Thus some researchers prefer the designation NAC (non-accommodating) to the designation FS for these neurons. Figure 6.3 illustrates the FS-type firing pattern. Most FS-type neurons tend to be somewhat "hair trigger" in their response to stimulus, which is to say that their repetitive firing pattern in response to a test stimulus does not exhibit a gradual transition to high firing rates.

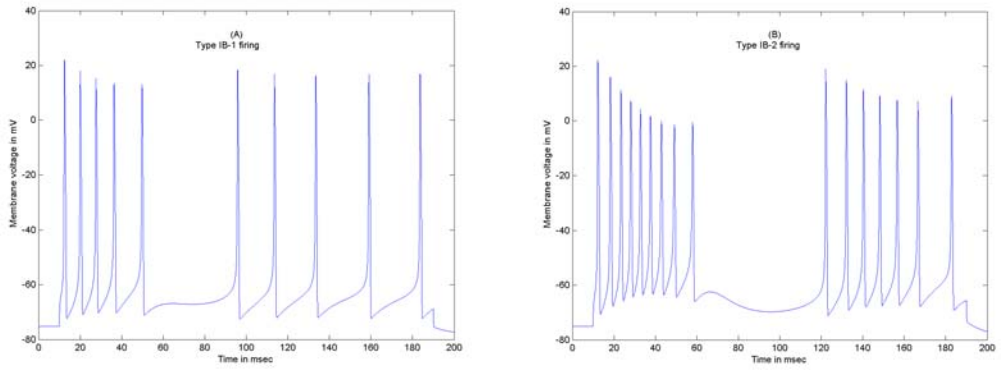


**(A)** **(B)**

**Figure 6.2:** IB-type firing patterns in response to injected current stimulus. (A) IB-1 type. (B) IB-2 type.

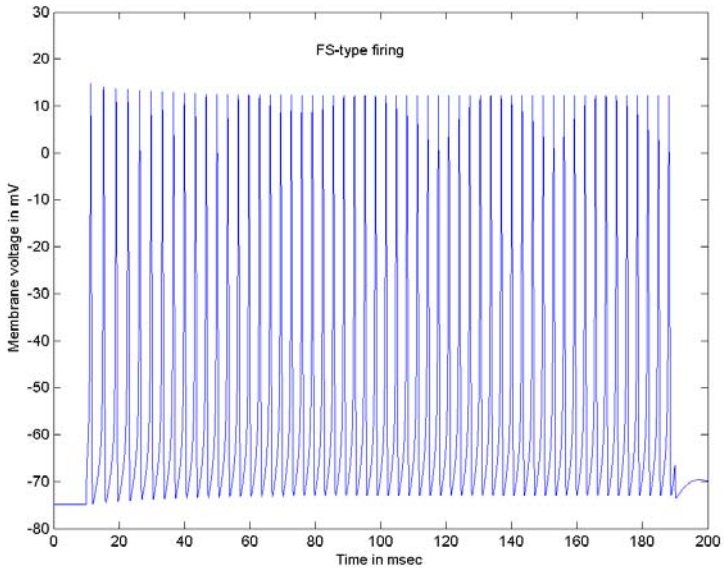


**Figure 6.3:** FS-type firing response to injected current stimulus.

As can be seen from Figure 6.3, the FS-type neuron's firing rate is significantly faster than that of the RS-type. Examination of the onset of the firing pattern has led to the distinguishing of three subclasses of FS-type response, called b-NAC, c-NAC, and d-NAC. Figure 6.3 illustrates the c-NAC (constant non-accommodating) subclass. The b-NAC subclass is characterized by a brief 3 to 5 spike very-high-frequency burst at onset which quickly settles into the constant steady-state firing pattern. It is not entirely clear what the mechanism is for this bursting-NAC response. The d-NAC or delayed-NAC response is characterized by a brief delay between the application of the stimulus and the onset of firing. There is an initial strong depolarization of the membrane voltage followed by a brief interval before AP spiking begins. Most likely this is caused by the presence in the trigger zone of a particular type of transient $K^+$ VGC known as the "A-current" or $I_A$ [McCO1]. Large basket cells (LBCs) and nested basket cells (NBCs) of different subspecies exhibit all three subclasses of NAC signaling. Bitufted cells (BTCs) and small basket cells (SBCs) have species exhibiting both d-NAC and c-NAC. Neurogliaform cells (NGCs) and Class-I chandelier cells (ChCs) are d-NAC FS-type cells, while Class-I Martinotti cells (MCs) are c-NAC FS-type cells [TOLE]. FS-type cells tend to make synapses to the soma or to the shafts of proximal dendrites at their target cells and will form synapses with any other type of cell. The exception to this rule is the Class-I NGC, which targets only axons.

About 17% of IINs in the neocortex are ***Class-II*** GABAergic cells. Some of these neurons exhibit a low spiking threshold and so are known as low threshold spiking (LTS) cells. Class-II cells are found in layers II-VI of the neocortex. The Class-II response shows adaptation during

tonic firing, and therefore is called an AC (accommodating) response. This is similar to the RS-type firing pattern except for two things. First, the firing rate is higher for AC-type than for RS-type. Second, the onset of accommodation is slower to appear than in the case of the RS-type cells. The AC signaling class also shows three subspecies, called b-AC, c-AC, and d-AC where the prefix designator means the same thing as above for the NAC class. Class-II NBCs have subspecies that exhibit all three firing subclasses. Class-II BTCs and MCs have subspecies that exhibit b-AC and c-AC signaling. Class-II LBCs have subspecies exhibiting d-AC and c-AC signaling. Class-II double bouquet cells (DBCs) exhibit c-AC signaling. The c-AC type is also sometimes called the RSNP (regular spiking non-pyramidal) type.

An interesting feature of LTS Class-II neurons (BTCs and MCs) is the exhibition of ***post-inhibitory rebound***. PIR is the firing of an AP spike upon release from hyperpolarizing inhibition. The mechanism for PIR is an inactivating low-threshold $Ca^{2+}$ VGC, commonly called a "T-current" or $I_T$. The $I_T$ channel is normally open at the cell's resting potential, and the resulting $Ca^{2+}$ current causes a slow depolarization of the cell's membrane potential, rising to the spiking threshold of the neuron. The neuron then fires an AP, in the process of which the $I_T$ channel is inactivated. The channel will not deactivate (release from the inactivation state) until the cell membrane is hyperpolarized, and will not activate again until the membrane recovers from hyperpolarization. LTS cells co-localize the neuropeptide SOM (somatostatin).

***Class-III*** IINs make up another 17% of all IINs in the neocortex. They co-localize the neuropeptide VIP (vasoactive intestinal peptide) and display an irregular spiking (IS) pattern [GIBS]. Some mathematical modelers refer to this as a 'chaotic' firing pattern [SHIL]. An illustration of an IS pattern is provided in [TOLE]. The Wilson models are not very successful at producing an IS pattern. They require an ad hoc sinusoidal oscillator to be added to the model dynamics to produce a chaotic response [WILS2, pp. 180-183]. Rulkov has demonstrated irregular (chaotic) spiking by his map-model neuron [SHIL]. Class-III IINs include DBCs, BPCs, and BTCs. Of these, vertically-oriented BPCs are the most common.

The three classes just described make up 84% of all IINs. The remaining 16% have not been given a specific classification, but their firing patterns can still be grouped into 3 major categories. Continuous bursting (CB) neurons respond to a constant stimulus of injected current with a burst firing pattern. This pattern is sometimes denoted as the BST class. Figure 6.4 illustrates the CB-type firing pattern of neurons in this class. Species of neurons exhibiting this firing pattern are found among the ChC, BPC, and DBC IIN cells.

Stuttering cells (STUT cells) make up a second interesting group of unclassified neurons. The STUT–type cells respond to a constant-current stimulus injection with high-frequency clusters of

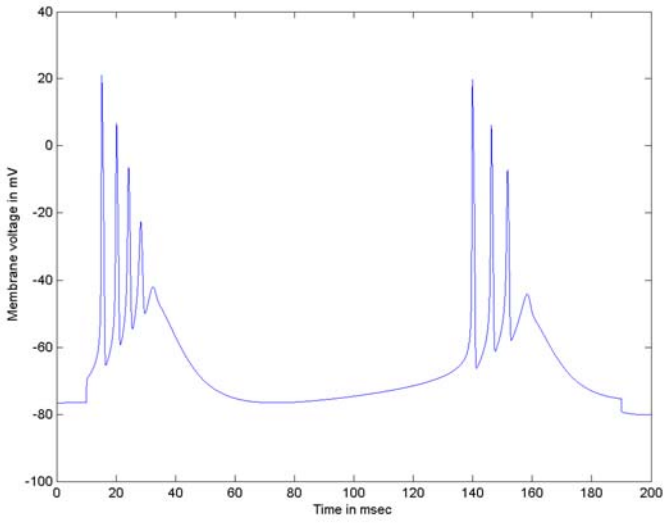


**Figure 6.4:** CB-type firing response to injected test current

APs, showing little or no accommodation, interspersed with periods of silence of unpredictable length. Some LBC, NBC, BTC, MC, and BPC neurons have subspecies of STUT-type cells. To date the modeling of STUT-type cells has not been very successful in that the unpredictability of the silent interval has not been successfully reproduced. [TOLE] provides an illustration of a STUT-type firing pattern.

Finally, some IINs exhibit an AC response to constant stimulus current injection yet do not fall under the Class-II designation. This is because Class-II classification uses a particular molecular category system, and IINs of the type we are now discussing do not fall into that molecular category. We will call them "other AC" (OAC) types. ChC, SBC, and BPC neurons exhibit subspecies that fall into the OAC-type category. For functional purposes, we can regard these as simply AC-type neurons and view them as a fast species of RS-type signaling.

The population percentages among CB-type, STUT-type, and OAC-type cells are not reliably known. The best we can presently say is that taken in total they add up to 16% of the total IIN population. Table II summarizes the mix of classifications that the various morphological IINs exhibit.

## § 2.3 The Wilson Model Schema

All five firing patterns exhibited in Figures 6.1 through 6.4 can be generated from a common modeling schema. Although Wilson's models are approximations of Hodgkin-Huxley membrane responses, the mathematical form producing these responses is not the typical sort of approximation one obtains by, for example, a curve fit or truncation of a Taylor series. Rather, the

**Table II: Classes of Inhibitory Neurons**

| Neuron | Class-I (NAC) | Class-II (AC) | Class-III (IS) | CB-type | STUT-type | OAC-type |
|---|---|---|---|---|---|---|
| SBC | X | | | ? | | X |
| NBC | X | X | | | X | |
| LBC | X | X | | | X | |
| DBC | X | | X | X | | |
| BPC | | | X | X | X | X |
| NGC | X | | | | | |
| BTC | X | X | X | | X | |
| MC | X | X | | | X | |
| ChC | X | | | X | | X |

X denotes that a subspecies of the neuron is found among the indicated types.
The Cajal-Retzius (CRC) cell is not classified. The CRC is found only in layer I.

equations for generating the model's response is the product of a specialized branch of mathematics known as ***nonlinear dynamics*** (NLD).

> One might argue that the ready availability of desktop microcomputers has made the study of nonlinear dynamics irrelevant: one need only approximate solutions of equations to study their behavior. This viewpoint rests on several major misconceptions, however. First, one is unlikely to have any idea what form the equations appropriate to a particular phenomenon might take without a grounding in nonlinear dynamics. Second, even when the relevant equations are already known, it is very difficult to determine how solutions depend on parameter values without knowledge of dynamical techniques. Finally, a knowledge of nonlinear dynamics is required if one is to be certain that one's computer approximations actually reflect the true dynamics of the system under study [WILS2, pg. 3].

In this introductory textbook, we will not be delving deeply into the mathematics and methods of NLD. Wilson's book [WILS2] provides an excellent introduction to this topic for the student interested in mastering its techniques. For present purposes, it is enough to remark that the model equations we are about to see are not arbitrarily chosen but, rather, deduced by means of NLD methods [WILS1].

The basic circuit model used by Wilson is shown in Figure 6.5 without synapses. Synaptic inputs are added in the standard manner described in chapter 3. Wilson's model incorporates four voltage-gated channel models. $G_{Na}$ and $G_K$ are the usual sodium and potassium channels. $G_{Ca}$ denotes a low-voltage calcium channel (a T-channel), while $G_H$ is a calcium-dependent potassium channel that produces after-hyperpolarization current $I_{K(AHP)}$. Wilson uses battery potentials $E_{Na}$ = 50 mV, $E_K = E_H = -95$ mV, and $E_{Ca} = 120$ mV. We can already see one approximation Wilson is making in his model schema, namely the use of a Nernst potential and standard conductance model for the calcium current rather than a GHK-equation-based expression for the calcium dynamics.

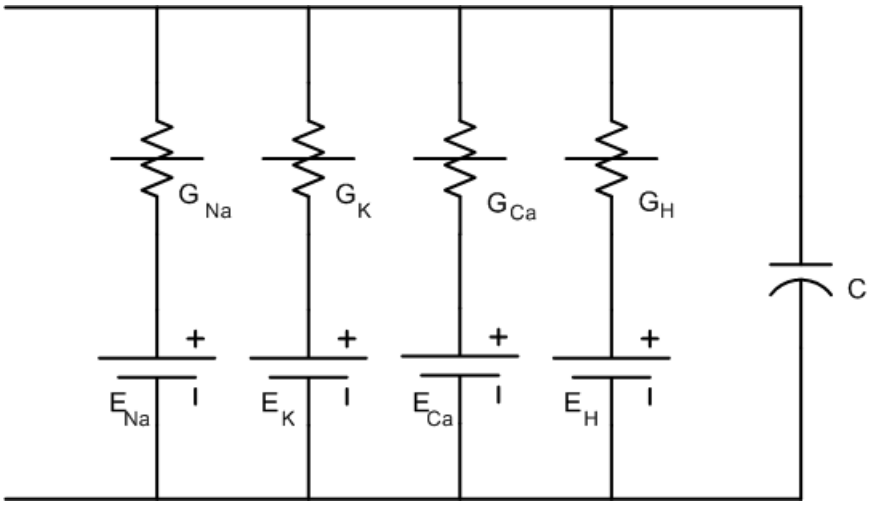


**Figure 6.5:** Circuit for the Wilson Model

When a stimulus current $I_s$, either due to synaptic action or to a test current stimulus, is injected into the cytoplasm (connected to the terminals at the left side of the figure), Kirchhoff's current law gives us the usual expression,

$$C\frac{dV_m}{dt} = -G_{Na}(V_m - 50) - G_K(V_m + 95) - G_{Ca}(V_m - 120) - G_H(V_m + 95) + I_s .$$

With conductances in μS and voltages in mV, the currents in this expression are in nA. The capacitance $C$ is in nF. Notice that there are no leakage terms in Wilson's model. Wilson accounts for the usual leakage terms by absorbing them into the expressions he will use for the voltage dependencies of the $Na^+$ and $K^+$ currents. This is possible because the empirical leakage potential values lie between $E_{Na}$ and $E_K$. Wilson describes this as "simply a matter of mathematical convenience" [WILS1]; it is the first novelty in his model, compared to our previous treatments.

The second novelty in Wilson's model, compared to our previous treatments, is introduced at the next step. Wilson introduces ***variable scaling*** into the membrane voltage equation. Variable scaling is a trick commonly used in numerical methods for solving differential equations. Its purpose is to minimize the impact of numerical roundoff and truncation errors in the computer calculations by making the terms multiplying the unknown ($V_m$ in this case) have less spread in the orders of magnitude of their values. In Wilson's case, he divides all the voltage terms by 100 and compensates for this by multiplying all the conductances and the capacitance by 100. Letting $v = V_m/100$, the result is

$$100 \cdot C\frac{dv}{dt} = -100 \cdot G_{Na}(v - 0.5) - 100 \cdot G_K(v + 0.95) - 100 \cdot G_{Ca}(v - 1.2) - 100 \cdot G_H(v + 0.95) + I_s .$$

Next Wilson chooses to make $C$ = 1 nF. This is primarily a matter of convenience for reducing the number of arithmetical operations required in the numerical solution for $v$. It has the physical consequence of implying a value for $C$ which is not a particularly biologically-realistic value. However, he will compensate for this by his choice of constants in the expressions for the conductance terms in order to force the solution to match measured data for the membrane voltage response. This is effectively the same as absorbing the ratios of the various $G_x/C$ values into the expressions for the voltage dependencies of these terms. It does, however, divorce the numerical value of the stimulus current from its empirical counterpart. If the real neuron has membrane capacitance $C_{act}$ and the laboratory test current stimulus is $I_t$, then the corresponding model stimulus current is $I_s = (C/C_{act}) \cdot I_t$. If $I_s$ is modeled as a synaptic conductance and synaptic potential, $G_{syn}$ and $E_{syn}$, then after voltage scaling one absorbs the capacitance value into $G_{syn}/C$. If the physiological channel conductance is $G_{act}$, then the model conductance is $G_x = (C/C_{act}) \cdot G_{act}$. Reported $C_{act}$ tend to fall in the range of ≈ 0.15 to 0.30 nF [YAMA], [McCO].

Wilson's next step applies nonlinear dynamics analysis to the experimentally-observed behavior of the membrane potential. He introduces four abstract variables, $m_\infty$, $R$, $T$, and $H$, to represent the voltage-dependencies of the four channel terms. These play functional roles similar to those of the Hodgkin-Huxley activation variables, although in Wilson's case they have no direct interpretation in terms of gating kinetics. He also introduces phenomenological constants $g_T$ and $g_H$ which are used to "tailor" the membrane voltage response to the different signal classes of neocortical neurons. These constants apply to the $G_{Ca}$ and $G_H$ terms in the voltage equation. These variables transform the membrane voltage equation into

$$\frac{dv}{dt} = -m_\infty \cdot (v - 0.5) - g_K R \cdot (v + 0.95) - g_T T \cdot (v - 1.2) - g_H H \cdot (v + 0.95) + I_s/100 . \quad (6.1)$$

Strictly speaking, the $I_s$ term is actually $I_s/100C$, but since $C$ = 1 in Wilson's model, this term need not be carried in the expression of (6.1). The numerical value of $I_s$ is related to the value of injected test current $I_t$ by the scaling rule noted above when $C$ is not equal to $C_{act}$.

The $m_\infty$ term in (6.1) represents the $Na^+$ VGC and is defined by

$$m_\infty = 17.8 + 47.6 \cdot v + 33.8 \cdot v^2 . \quad (6.2)$$

The leading constant term is regarded as a leakage term for $Na^+$. The overall form of (6.2) was chosen to allow class-I spiking behavior in the neuron, i.e. arbitrarily low spiking rates. The "∞" subscript is intended to denote a very fast channel time constant relative to the time constants for the other channel terms in the overall model. In effect, the $Na^+$ VGC is modeled as responding

instantly to changes in membrane voltage.

When (6.2) is inserted into (6.1), the result is a cubic functional dependency for the $Na^+$ current. A cubic dependency is maintained for all the other terms as well, and this is done for purposes of analytic tractability in the NLD analysis of (6.1). This is a mathematical rather than a physiological constraint Wilson places on the model, and it ties back to much earlier work in the development of the mathematics of NLD pioneered by FitzHugh [FITZ] and Nagumo [NAGU]. The physiological consequence of this decision is that the Wilson models cannot simulate channel inactivation. The production of inactivation dynamics minimally requires $5^{th}$-order polynomial dependencies in the terms in (6.1), which both increases the computational cost of the model and makes its analysis more difficult. Therefore, *there are some neuronal phenomena that are not accurately modeled by Wilson's models.* Two of the more prominent of these are representation of the refractory period and the post-inhibitory rebound dynamic [WILS1].

The $g_K$ term in (6.1) is set equal to the constant value $g_K = 26$ for all four signaling types of Wilson models. Potassium VGC dynamics are captured in the $R$ term, which is defined by the differential equation

$$\begin{aligned} &\frac{dR}{dt} = \frac{1}{\tau_R}\left(-R + R_\infty\right) \\ &R_\infty = 1.24 + 3.7 \cdot v + 3.2 \cdot v^2 \end{aligned} \quad . \tag{6.3}$$

The constant term in the expression for $R_\infty$ takes in the potassium leakage current. The time constant $\tau_R$ in the model is truly a constant, in contrast to the case in Hodgkin-Huxley models. The value used for the time constant depends on which signaling class (RS, FS, IB, or CB) is being represented. Again we have an overall cubic nonlinearity in (6.1) from this term, so the model can not represent any inactivation dynamics for $K^+$ VGCs.

The $g_T$ term in (6.1) is a constant that depends on the signaling type being represented. The low threshold $Ca^{2+}$ VGC dynamic is determined through the $T$ function, which is defined by

$$\begin{aligned} &\frac{dT}{dt} = \frac{1}{\tau_T}\left(-T + T_\infty\right) \\ &T_\infty = 8 \cdot \left(v + 0.725\right)^2 \end{aligned} \quad . \tag{6.4}$$

In this case, the time constant is set to the same value, $\tau_T = 14$, for all neuronal signaling classes. We again have the cubic nonlinearity in (6.1), and this prevents the representation of inactivation for the low voltage calcium channel. It is this limitation that prevents the representation of the post-inhibitory rebound phenomenon in Wilson's models.

Finally, the $Ca^{2+}$-dependent $K^+$ VGC is represented by parameter $g_H$, the value of which

depends on the signaling type being represented, and the *H* function

$$\frac{dH}{dt} = \frac{1}{\tau_H}\left(-H + 3 \cdot T\right) . \qquad (6.5)$$

The time constant $\tau_H = 45$ is the same for all signaling classes. What is interesting to note in (6.5) is the way in which the *H* function incorporates the $Ca^{2+}$ dependence by merely scaling the *T* variable. Increasing the value of *T* increases the slope *dH*/*dt* (makes it more positive), and this reflects the activating influence of cytoplasmic free $Ca^{2+}$ on these $K^+$ VGCs. The cubic dependency of the *H* channel is introduced indirectly through its dependence on the *T* variable.

Equations (6.1) through (6.5) completely describe Wilson's modeling schema. Different signaling classes of neurons are represented by the choice of just three parameters:

| | | | |
|---|---|---|---|
| **RS Type:** | $g_T = 0.1$; | $g_H = 5$; | $\tau_R = 4.2$ (ms) |
| **FS Type:** | $g_T = 0.25$; | $g_H = 0$; | $\tau_R = 1.5$ (ms) |
| **CB Type:** | $g_T = 2.25$; | $g_H = 9.5$; | $\tau_R = 4.2$ (ms) |
| **IB-1 Type:** | $g_T = 0.8$; | $g_H = 4$; | $\tau_R = 4.2$ (ms) |
| **IB-2 Type:** | $g_T = 1.2$; | $g_H = 3.4$; | $\tau_R = 4.2$ (ms) |

The numerical values given above are the direct values used in the actual simulation calculations for computer solution of the model equations. In the modeling equations time is in ms. With Wilson's choices of NLD parameters the neurons have a resting potential of around –74.8 mV ($v = -0.748$) and a firing threshold of around –60 mV. In his 1999 paper [WILS1], Wilson comments that decreasing $\tau_T$ and $\tau_H$ by "about a factor of three" will also provide "a much better fit" to the firing pattern of chattering pyramidal cells [GRAY1]. However, doing this does not by itself result in a firing pattern that matches the chattering response shown in [GRAY1] very well at all. The selection of parameters that will result in firing patterns other than the five basic types is not an easy task.

## § 3.0 The Izhikevich Model Schema

Wilson's models have considerably less computational cost than the Hodgkin-Huxley model. This cost reduction is paid for by the loss of some biological accuracy in the representation of the neuron, as we have seen. It is not too difficult to understand what produces the loss of physiology details in the Wilson modeling schema, and thereby to be forewarned about what sort of signaling will be simulated inaccurately in a neural network model. Wilson's models remain close enough to actual neural physiology to have a meaningful circuit representation. The same is not true of our next example.

Although Wilson's models represent a considerable improvement over Hodgkin-Huxley so far

as the computational cost is concerned, they are still expensive enough to limit their practical use to relatively small networks of neuron cell groups. As inhibitory and excitatory synapses are added to the model, the model accrues additional differential equations in pairs (two more equations for an excitatory synapse, two more for an inhibitory synapse), taking it from four differential equations up to at least eight for a minimal neuron with network synaptic connections. This is still a cost improvement in comparison to models such as the McCormick-Huguenard model of thalamocortical relay neurons, which would expand from ten to fourteen differential equations when excitatory and inhibitory synaptic connections are added. The Wilson schema also benefits from the simpler form of its auxiliary equations, which are polynomials and do not involve computing exponential functions. But the Wilson schema simplification returns less than an order of magnitude reduction in computational costs. Thus, its practical application to neural network modeling is limited to small networks ("netlets") containing on the order of tens of neurons and computation time climbs rapidly with each additional neuron added to the network.

To simulate larger neural networks, containing thousands of neurons, additional computational simplification is needed. This is bought at the price of the outright loss of any immediate connection to the biological mechanisms that constitute the basis of one's physical understanding of neuronal behavior. Thus, the modeling methods we now turn to are typically not favored by physiologists but they are, for obvious reasons, popular with neural network theorists.

Our next example is a model schema developed by Izhikevich [IZHI1]. Like Wilson's models, Izhikevich's models are the product of the techniques of nonlinear dynamics. Unlike Wilson's models, the abstraction made from channel conductance mechanisms and Nernst potentials is complete. There is, consequently, no meaningful circuit model representation for the Izhikevich neuron.

The Izhikevich modeling schema is represented by only two differential equations,

$$\begin{aligned} \frac{dv}{dt} &= 0.04 \cdot v^2 + 5 \cdot v + 140 - u + I \\ \frac{du}{dt} &= a \cdot (b \cdot v - u) \end{aligned} \tag{6.6}$$

where $v$ is a variable taken to represent the membrane voltage and $I$ is an input variable taken to represent either a test current stimulus or synaptic inputs to the neuron. Variable $u$ is called the "membrane recovery variable" and is used for re-setting the spikes generated by the $v$ equation. The $v$ equation is scaled such that the numerical value of $v$ can be regarded as a membrane potential in mV, and the variable $t$ is interpreted as time in ms. Equations (6.6) are accompanied by an auxiliary "reset" condition,

$$\text{if} \quad v \geq +30\,\text{mV}, \quad \text{then} \begin{cases} v = c \\ u = u + d \end{cases} . \tag{6.7}$$

Variables *a*, *b*, *c*, and *d* are numerical parameters that determine what kind of spiking behavior will be produced by the neuron when subjected to a step-like test stimulus, *I*.

The Izhikevich schema is capable of producing a large "library" of spiking responses. Twenty example spiking patterns, all generated from (6.6)-(6.7) using different selections for {*a*, *b*, *c*, *d*}, are illustrated in [IZHI2]. Parameter "recipes" for six different signaling types have been catalogued in [IZHI1]. He reports RS, FS, and IB signaling models plus a chattering cell mimic (CH), a low-threshold-spiking mimic (LTS), and a "thalamocortical" type (TC). Parameters for these are shown in Table III.

While we might say that Wilson's models represent an intermediate step between the "mechanism" representations of Hodgkin-Huxley models and the pure "function" representations of abstract neural networks, Izhikevich's modeling schema is entirely functional in its representation. Furthermore, since the model abandons physiological representation of mechanisms, a suitable choice of synaptic weight vector *W* (see chapter 4) can be made so that the representation of synaptic connections to the neuron can be reduced to a single differential equation that represents action potential input impulses by a single time constant, exponentially decaying "current" pulse. Thus it is possible to "cap" the number of differential equations to be solved to as few as three per neuron. Izhikevich estimates that his model is almost two orders of magnitude less expensive to compute than a minimal Hodgkin-Huxley model.

The Izhikevich models produce signaling patterns that are qualitatively similar to spiking patterns experimentally observed in biological neurons. No *quantitative* physiological significance attaches to any of the models' parameters or variables, although in his papers Izhikevich often writes in a manner such as to suggest an attribution is possible. It is not. While the modeling schema does a credible job of capturing signaling responses to test current stimulus, it does not capture the refractory period effects exhibited in biological neurons. Refractory behavior is postulated by some theorists to be an important element in signal filtering in networks and thus tied in with the need to mimic firing patterns; at present this is still merely conjecture.

**Table III: Izhikevich Parameters for Six Signaling-type Models**

| Signaling-type | a | b | c | d |
|---|---|---|---|---|
| RS | 0.02 | 0.20 | –65 | 8 |
| FS | 0.10 | 0.20 | –65 | 2 |
| IB | 0.02 | 0.20 | –55 | 4 |
| CH | 0.02 | 0.20 | –50 | 2 |
| LTS | 0.02 | 0.25 | –65 | 2 |
| TC | 0.02 | 0.25 | –65 | 0.05 |

## § 4. Other Abstract Neuron Models Described by Differential Equations

At the time of this writing, the Izhikevich modeling schema is the latest in a line of abstract neuron models described by differential equations. For purposes of completeness, it is worthwhile to take a little time to mention three older models, all of which are considerably more computationally expensive than the Izhikevich modeling schema and in this sense are now obsolete. The oldest of these we have already mentioned briefly, namely the FitzHugh-Nagumo model [FITZ], [NAGU]. It is described by two polynomial equations, one of which is a cubic polynomial. It is a functional model with no easily-definable connection to biological mechanisms. The second, which was for a time very popular, is the Morris-Lecar model [MORR]. Similarly to Wilson's models, the Morris-Lecar model retains something of a direct connection to physiological mechanisms and can be meaningfully represented by a circuit model. Its computational complexity is somewhat greater than the Wilson modeling schema, and so is more expensive to compute. It has the further handicap of being able to represent fewer signaling types. Finally, the Rose-Hindmarsh model [RoHi] is an NLD-based model described by three differential equations. It is a very versatile model capable of representing a number of signaling types. Its computational cost is slightly less than that of Wilson's schema but considerably higher than that of Izhikevich's schema.

## § 5. The Rulkov Modeling Schema

All the modeling schemas discussed to this point are based on differential equations and must be converted to difference equation form before they can be simulated on the computer. Our last abstract neuron model, the Rulkov modeling schema [RULK1], differs in kind from these. It is called a ***map-based model***, which means only that it is developed in difference equation form from the very beginning. Like Izhikevich's and Wilson's modeling schemata, it is the product of the mathematics of nonlinear dynamics. Like Izhikevich's schema, no quantitative physiological significance can be attached to any of its parameters or variables.

Difference equations are not differential equations, and a difference equation can be said to be "equivalent" to a differential equation only under particular conditions of restriction. This means that all neural network simulations, which must always use difference equations, are in principle open to the question of to what degree they can faithfully replicate what is going on in a real neural network, for which time is a continuous, not a discrete, parameter. One of the most important issues is how one knows one's difference equation representation will not "miss" generating an action potential because its simulation time steps are quantized. A related issue is the question of whether and how discretization of the time steps in a simulation affects the overall

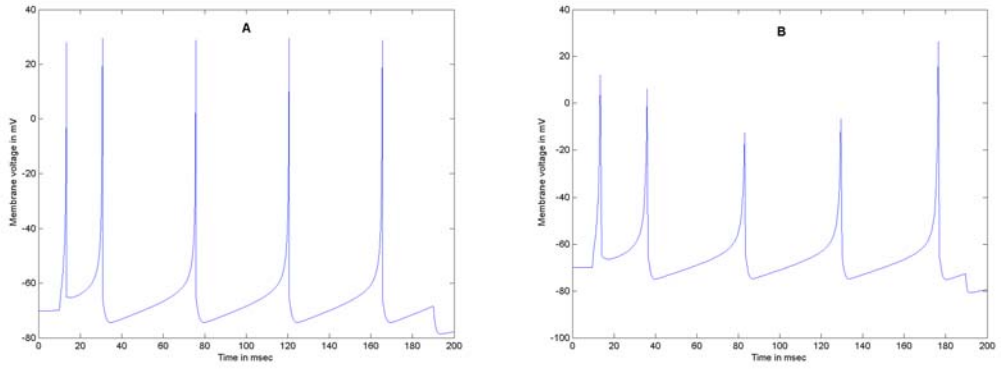


**Figure 6.6:** Effect of time step $\Delta t$ on the response of the Izhikevich RS model. (A) $\Delta t$ = 0.01 ms. (B) $\Delta t$ = 0.5 ms. In addition to the obvious differences in pulse amplitudes, note the significant changes in pulse times. The stimulus was a step of amplitude $I$ = 10.0 turned on at $t$ = 10 ms and off at $t$ = 190 ms.

population responses in a large neural network containing feedback from "downstream" neurons back to the "upstream" neurons whose signaling pathways drive the former.

Figures 6.6 illustrate the step size issue for the case of Izhikevich's RS neuron model. Figure 6.6(A) was simulated using Euler's method and a time step of 0.01 ms; figure 6.6(B) was simulated under the same conditions except that a time step of 0.5 ms is used. The differences in pulse amplitudes between the two figures are obvious, but this is not the most important difference between the figures. Of far more importance in the context of neural network modeling is the difference in the times when spiking occurs. What has happened is that the difference equation for $\Delta t$ = 0.5 ms is no longer an accurate representation of Izhikevich's differential equations. In effect, one is left with "different" neuron models in the two figures. When (6.6) is converted to difference equation form using Euler's method, avoidance of excessive sensitivity to $\Delta t$ requires that $\Delta t$ be made no larger than 0.01 ms.

Map-based methods avoid this issue by developing the desired signal-type response in difference equation form at the outset. The price paid for this is that for these models $\Delta t$ is now fixed and cannot be varied once the modeling parameters are established. A second disadvantage is that map-based models are developed in terms of an "iteration index" rather than a "time index" and so the effective value of $\Delta t$ is usually not evident during the model development. This is illustrated in [RULK2], where Rulkov originally presented his modeling schema. In order to correlate the model's iteration index against a real time parameter, it is necessary to compare the map-based model result against a physiological comparand, typically a Hodgkin-Huxley model. Rulkov et al. [RULK1] report that one time step in simulation corresponds to "about 0.5 ms"; a closer examination of the model puts the equivalence at 0.495 ms [CHENG].

The benefits accrued by this method are that it can be guaranteed the model will not miss any

spiking events and it requires 50× fewer iterations for a given real time simulation span. This leaves only the question of whether or not time quantization affects large-scale network behavior in the presence of feedback. In a biological system, a spiking event can occur at any time; in a simulation model it can occur only at one of the simulation time steps. Simulation studies of multiple, asynchronous synaptic input responses using physiological neuron models indicate that neuronal response is relatively unaffected by the arrival of asynchronous synaptic inputs, compared to perfectly synchronous ones, provided the time spacing between synaptic events is no greater than about 0.5 ms and time constants for synaptic current decay are no less than 2 ms [POOL]. While this does not constitute a general proof of the proposition, one may conclude that time steps of 0.5 ms or less leave overall network behavior unaffected provided the neuron models themselves are unaffected by discrete time steps of this magnitude. The Rulkov models meet this criterion.

## § 5.1 Rulkov's Map Schema

Turning now to the modeling schema itself, the Rulkov schema employs a base model comprised of two difference equations [RULK1-2, SHIL],

$$\begin{aligned} x_{n+1} &= f_\alpha\left(x_n, x_{n-1}, y_n + \beta^e \cdot I_n^{syn}\right) \\ y_{n+1} &= y_n - \mu\cdot\left(x_n + 1\right) + \mu\cdot\sigma + \mu\cdot s^e \cdot I_n^{syn} \end{aligned} \tag{6.8}$$

where the auxiliary function is defined as

$$f_\alpha\left(x_n, x_{n-1}, u\right) = \begin{cases} u + \left(\alpha/\left(1 - x_n\right)\right), & x_n \le 0 \\ \alpha + u, & 0 < x_n < \alpha + u \text{ and } x_{n-1} \le 0 \\ -1, & x_n \ge \alpha + u \text{ or } x_{n-1} > 0 \end{cases} . \tag{6.9}$$

In these expressions $n$ is an integer denoting the time index of the simulation. The corresponding time is $t = n \cdot \Delta t$, with $\Delta t = 0.495$ ms. Variable $x_n$ is usually called "the fast variable" in nonlinear dynamics, and in this case it corresponds to (but does not equal) the membrane potential of the neuron. Variable $y_n$ is called "the slow variable" and has no physiological correspondent. $I_n^{syn}$ is the variable representing synaptic input currents (or an externally-applied test stimulus) but does not numerically correspond to a physiological value for synaptic current (i.e., it is "functional" rather than "mechanistic"). $\beta^e$ and $s^e$ are scaling factors for weighting the external input variable.

The other variables in (6.8)-(6.9) are the model parameters. Different choices for $\alpha$, $\mu$, and $\sigma$ define different firing patterns made to correspond to the signaling types for the particular class of neuron being modeled. Using a two-compartment Hodgkin-Huxley model developed by Mainen

and Sejnowski [MAIN], Rulkov et al. obtained parameters for an RS-type model and an IB-type model [RULK1]. The parameters and the associated test stimulus amplitude, $I_{\max}$, for $I_n^{syn}$ shown in Table IV reasonably reproduce the firing patterns shown in [RULK1].[2]

**Table IV: Model Rulkov RS- and IB- Parameters**

| Neuron | $\alpha$ | $\mu$ | $\sigma$ | $\beta^e$ | $s^e$ | $I_{\max}$ |
|---|---|---|---|---|---|---|
| RS | 3.65 | $5{\cdot}10^{-4}$ | 0.06 | 0.133 | 1.0 | 0.03 |
| IB | 4.1 | $5{\cdot}10^{-4}$ | -0.036 | 0.330 | 1.0 | 0.015 |

Rulkov's schema has the interesting peculiarity that the input "current" stimulus is actually applied to the slow variable, $y_n$, rather than the "membrane voltage" variable, $x_n$. The role of $\beta^e$ in the model is primarily to produce *accommodation* in the step-input response of the RS- and IB-type neuron models. $\beta^e = 0$ suppresses accommodation in the spiking response. Note, too, that the calibrated Rulkov signaling responses use different stimuli, $I_{\max}$, for the two different cases.

The action potential response of the neuron is not given directly by either $x_n$ or $y_n$. Letting $z_n$ denote the AP response of the neuron ($z_n = 1$ denoting an AP, $z_n = 0$ denoting no AP), the firing condition for the neuron is

$$z_n = \begin{cases} 1, & x_n \geq \alpha + y_n + \beta^e \cdot I_n^{syn} \quad \text{or} \quad x_{n-1} > 0 \\ 0, & \text{otherwise} \end{cases} . \tag{6.10}$$

Note that the condition for $z_n = 1$ is the same as the condition corresponding to $x_{n+1} = -1$ in (6.9).

The Rulkov FS-type neuron is developed as a special case modification of the base model. He introduces a "hyperpolarization current" term, analogous to hyperpolarizing VGCs in a biological neuron, of the form

$$I_{n+1}^{hp} = \gamma^{hp} \cdot I_n^{hp} - g^{hp} \cdot z_n \tag{6.11}$$

where $\gamma^{hp}$ and $g^{hp}$ are two new model parameters. $\gamma^{hp}$ controls the decay time constant of the "hyperpolarizing current" and $g^{hp}$ sets the maximum amplitude of this "current." Note that $I_{n+1}^{hp}$ depends on the present firing state, $z_n$, of the neuron. (6.11) replaces the slow variable equation for $y_n$ in (6.8) and the equation for $x_n$ is modified to

$$x_{n+1} = f_\alpha\left(x_n, x_{n-1}, u = y^{rs} + \beta^{hp} \cdot I_n^{hp} + \beta^e \cdot I_n^{syn}\right) . \tag{6.12}$$

[2] The parameters reported in [RULK1] for the IB neuron model do not reproduce the firing pattern shown there.

Here $y^{rs}$ and $\beta^{hp}$ are two additional model parameters denoting a resting state variable and a hyperpolarization scaling factor, respectively. The function $f_\alpha$ is unchanged from (6.9). The action potential firing condition for the FS-type model remains $z_n = 1$ if $x_n \geq \alpha + u$ or $x_{n-1} > 0$, and $z_n = 0$ otherwise. Rulkov's parameter values for the FS-type neuron model are:

**Rulkov FS-type Model** $\alpha = 3.8$; $\beta^e = 0.1$; $y^{rs} = -2.9$; $\beta^{hp} = 0.5$; $\gamma^{hp} = 0.6$; $g^{hp} = 0.1$; $I_{\max} = 0.016$.

Synaptic inputs to the neuron are modeled as geometrically decaying pulses. Separate difference equation parameters are used for excitatory vs. inhibitory synapses, adding two more difference equations to the neuron model (for a minimum of four difference equations). Let $S_n^e$ denote the weighted sum of all AP inputs at excitatory synapses at time index $n$,

$$S_n^e = \sum_{j=1}^{J_e} w_j \cdot z_n^{(j)} \tag{6.13}$$

where $w_j \geq 0$ is the synaptic weight of the $j^{th}$ synapse, $z_n^{(j)}$ is the firing state of the $j^{th}$ presynaptic neuron, and $J_e$ is the total number of presynaptic cells sending excitatory signals to the neuron. Note that $S_n^e = 0$ if no presynaptic cell is firing an AP. The excitatory stimulus is then given by

$$I_{n+1}^{syn(e)} = \gamma \cdot I_n^{syn(e)} - g_{syn} \cdot \left(x_n - x_{rp}\right) \cdot S_n^e \quad . \tag{6.14}$$

Here $\gamma$ controls the time constant of the decay of the stimulus and $g_{syn}$ is a global scaling factor determining the maximum excitatory stimulus into the neuron. $x_{rp}$ is a parameter analogous to $E_{syn}$ in the Hodgkin-Huxley model. Rulkov et al. model the excitatory synaptic input using $x_{rp} = 0$. Since $x_n < 0$ except when the neuron is firing an AP, the second term in (6.14) results in a depolarizing stimulus.

For inhibitory inputs, the variables $S_n^i$ and $I_n^{syn(i)}$ are given by (6.13) and (6.14) merely by changing the *e* superscripts and subscript to *i* superscripts and subscript, with the obvious re-interpretation of the presynaptic variables and weights (with $w_j > 0$). For inhibitory synapses Rulkov uses $x_{rp} = -1.1$. In the network simulations reported in [RULK1], the synaptic "time constant" variables were $\gamma = 0.6$ and $\gamma = 0.96$ for excitatory and inhibitory synapses, respectively. The total stimulus input to the neuron is given by

$$I_n^{syn} = I_n^{syn(e)} + I_n^{syn(i)} \tag{6.15}$$

subject to the constraint $-0.0001 < \beta^e \cdot I_n^{syn} < 0.1$, which is imposed to keep the dynamics of the model within the valid range set by Rulkov's NLD derivation.

Equation (6.14) dictates that the natural response of the stimulus follows a geometric decay governed by the geometric ratio $\gamma$. Bearing in mind that $n$ is a simulation step index and not a time index, the geometric ratio can be related to the decay time constant $\tau$ we discussed in the earlier chapters by requiring that one simulation step correspond to the ratio of $\Delta t$ to $\tau$,

$$\gamma = \exp(-\Delta t/\tau) \Rightarrow \tau = \Delta t/\ln(1/\gamma).$$

With $\Delta t$ = 0.495 ms for the Rulkov model, the geometric ratios given above correspond to physiological time constants of 0.969 ms and 12.1 ms, respectively, which are in the biologically-reasonable range for postsynaptic currents in AMPA and $GABA_A$ synapses [SILV].

## § 5.2 Neurodynamics of the Rulkov Modeling Schema

Like Izhikevich's model, the Rulkov model is capable of generating a much larger suite of responses than merely the three neuron signaling types parameterized in the previous section. In addition, there are a variety of sub-types within the major classifications for RS, IB, FS, and CB neurons. For example, Rulkov's models in the previous section do not correspond to either Wilson's or Izhikevich's models for RS, FS, and IB neurons. For both these reasons, it is commonplace for the modeler to need to come up with parameter values different from those tabulated above. This is not particularly easy to do even if one is well-trained in the NLD methods from which the Rulkov modeling schema is derived. Some basic understanding of what controls general features of the model dynamics is necessary in order to find new or different Rulkov signaling responses.

The starting point for understanding the basic dynamics of the system defined by (6.8) is the case where the model does not exhibit accommodation in its response to constant current stimulus. This is the $\beta^e = 0$ case. For constant-valued $I_n^{syn}$, we can make the substitution

$$\sigma_c \overset{\Delta}{=} \sigma + s^e \cdot I_n^{syn}$$

and examine the basic dynamics of the system in terms of this excitation variable [RULK2], [SHIL]. We first examine the conditions under which the model possesses a steady-state solution for $\sigma_c$. In nonlinear dynamics, such a solution is called a ***fixed point***. In the steady-state, $x_{n+1} = x_n$ and $y_{n+1} = y_n$. Substituting these conditions into (6.8) and (6.9), we find that the fixed point solution is given by

$$\begin{aligned} x &= \sigma_c - 1 \\ y &= x - \frac{\alpha}{1-x} \end{aligned} \quad . \tag{6.16}$$

The pair ($x$, $y$) given by (6.16) is a fixed point solution but it is not necessarily a *stable* fixed point solution. For some solutions ($x$, $y$), any tiny perturbation to this solution may carry the system away from the fixed point. Such fixed points are called *unstable* fixed points. Determining if a fixed point is stable or unstable calls upon what is known as a ***homocline analysis*** by NLD theorists. The details of such an analysis are beyond the scope of this textbook, but the outcome of this analysis for the case of Rulkov's equations are simple to state. In the region of small $\mu$, the solution (6.16) is a stable fixed point if and only if

$$\sigma_c < 2 - \sqrt{\alpha/(1-\mu)} \ . \tag{6.17}$$

The value $\sigma_{th} = 2 - \sqrt{\alpha/(1-\mu)}$ is called a ***bifurcation value*** and it represents the ***firing threshold*** of the model neuron. The neuron will not produce spike outputs for values of $\sigma_c$ in the range given by (6.17).

For $\sigma_c > \sigma_{th}$, the neuron will produce spiking outputs. Here two possible cases must be considered. The neuron's spiking response may either be ***tonic*** or ***bursting***. A tonic response is the type of response produced, for example, by a biological FS-type neuron excited by a constant current stimulus. Likewise, an RS-type neuron similarly excited produces tonic firing once its accommodation dynamics have completed (refer to figure 6.1). A bursting response is the signaling type produced by IB-type and CB-type neurons. Rulkov has shown that for $\alpha < 4$, the neuron can only produce tonic firing when $\sigma_c$ exceeds the threshold value. For $\alpha > 4$, the neuron may produce either tonic or bursting responses depending on the specific value of $\sigma_c$. The parametric boundary region separating these two cases is determined by simulation studies for the Rulkov model.

Figure 6.7 summarizes the above. This type of diagram is called a ***bifurcation diagram*** and delineates different regions of nonlinear behavior in the model system. The blue boundary shown in the figure is the threshold boundary and separates the non-spiking and spiking regions. The red line separates the tonic spiking (below and to the right of the red line) and the bursting region (above and to the left of the red line, and above and to the right of the blue line).

Consider the case where $\alpha < 4$ and $\sigma_c$ places the system to the left of the threshold boundary. The neuron in this case produces no spiking response (no action potential). Now suppose an applied stimulus changes $\sigma_c$ such that the system moves to the right of the threshold boundary. The neuron then begins to produce action potential spikes in a tonic firing mode and continues to do so until $\sigma_c$ returns to the region to the left of the threshold boundary.

Next consider the case where $\alpha > 4$ and $\sigma_c$ places the system to the left of the threshold line. In

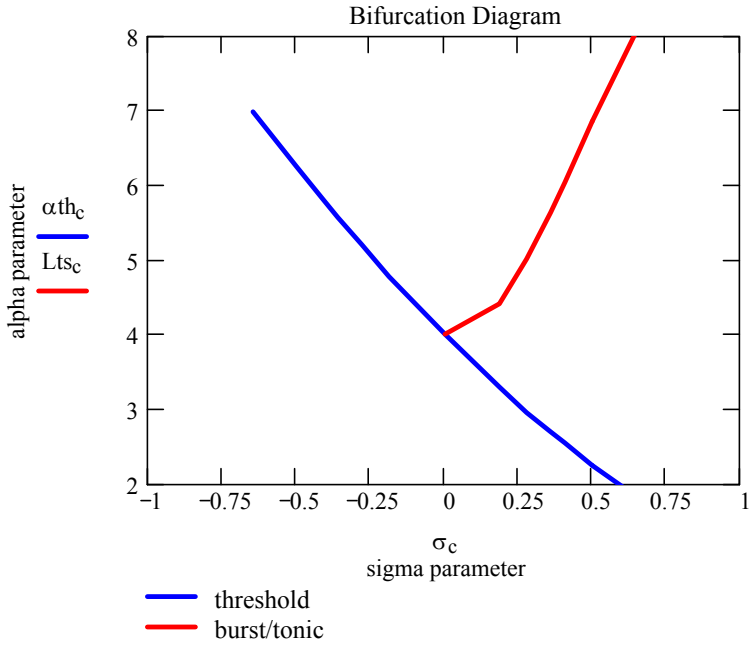


**Figure 6.7:** Bifurcation diagram describing the dynamics of the Rulkov model. The blue line is given by (6.17) and represents equality between the left- and right-hand sides of (6.17). For parameters ($\alpha$, $\sigma_c$) to the left and below the blue line, the neuron is below threshold and the fixed point is stable (produces no spiking). For ($\alpha$, $\sigma_c$) to the right and above the blue line, either tonic spiking or burst spiking results. The tonic spiking region is below and to the right of the red line, which depicts the tonic-bursting parameter boundary.

this case, the neuron again produces no AP spikes. However, now when an applied stimulus changes $\sigma_c$ such that the system moves to the right of the threshold boundary, one of two responses will result. If $\sigma_c$ places the system in the burst-firing region, the neuron responds with a burst of two or more AP spikes. If $\sigma_c$ places the system in the tonic-firing region, the neuron responds with a tonic firing pattern.

It is important to understand that during simulations the slow variable, $y$, changes much more slowly than the fast variable, $x$, and so the neuron passes through regions where it is not at a fixed point. This dynamic cannot be seen from the bifurcation diagram; to examine this requires what is known as a ***phase plane diagram***. Note that the coordinates in figure 6.17 are not ($x$, $y$). In order to use figure 6.7, it is important to bear in mind that the transient nonlinear dynamics of the neuron are not depicted by this figure. To see what the response actually is, one runs the simulation. Furthermore, the transient effect of neither the accommodation variable, $\beta^e$, nor the slow variable parameter, $\mu$, are represented in the bifurcation diagram. Figures 6.8 illustrate the responses of the RS- and IB-type models for the parameters provided in Table IV. One curiosity of the nonlinear dynamics worth noting for these models is this. The slow-variable parameter $\mu$, which controls the rate of change of $y$, also affects the burst response of the IB-type neuron. If the

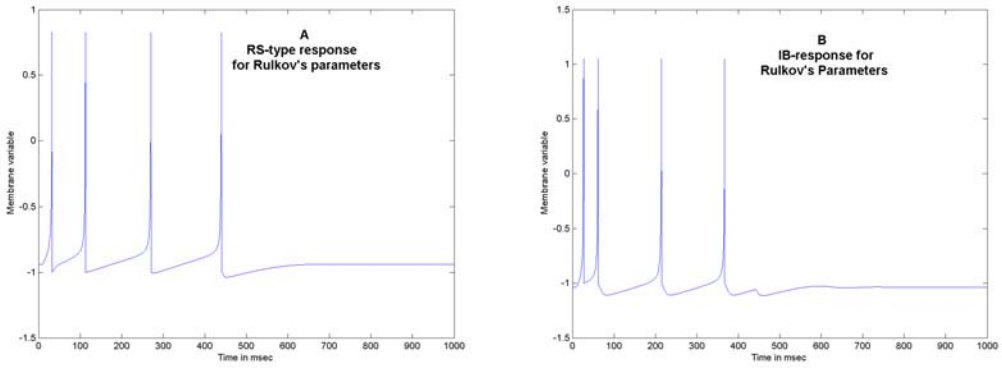


**Figure 6.8:** Rulkov RS- and IB-neuron responses to constant current stimulus. The stimulus was applied at $t$ = 10 ms and turned off at $t$ = 440 ms.

parameter $\mu$ is increased to 0.001, with all other parameters in Table IV held the same, the second spike in the IB-neuron response disappears and the neuron exhibits non-accommodating spiking (that is, it does not burst at this input stimulus setting). This demonstrates that some coupling exists between $\mu$ and $\beta^e$ in the nonlinear dynamics of the model. However, these two variables do have differing effects and one must not regard them as "interchangeable" in coming up with modeling parameters. Unfortunately, no "rules" or guidelines for selection of these parameters was given by Rulkov et al., nor did they describe the procedure by which they arrived at their published model parameters. Thus, there is a certain amount of art, and a certain amount of trial and error, involved in coming up with a complete set of model parameters using the Rulkov modeling schema.

There is another important point to mention in regard to the neurodynamics of the Rulkov model. Most nonlinear systems, including the Rulkov model system, have regimes of operation where the system evolves to a ***limit cycle*** response (a non-terminating, sometimes periodic, time evolution for which no fixed point solution is obtained). The production of a limit cycle response depends in part on the model parameters, but it also can depend on the initial conditions for the $x$ and $y$ variables at the beginning of the simulation. This is so in the case of the Rulkov model. Therefore, **at the beginning of a simulation the initial conditions ($x_0$, $y_0$) should be set equal to the fixed-point solution (6.16)**.

Figure 6.9 illustrates the Rulkov FS- response. In the case of the FS-type neuron, non-accommodating, tonic firing is the desired response to stimulus, and thus for this model $\alpha < 4$ is used. **Initial conditions for the FS-type neuron differ from those of the base model**. An adequate initial condition is provided by $x_0 = -1$ and $I_0^{hp} = 0$.

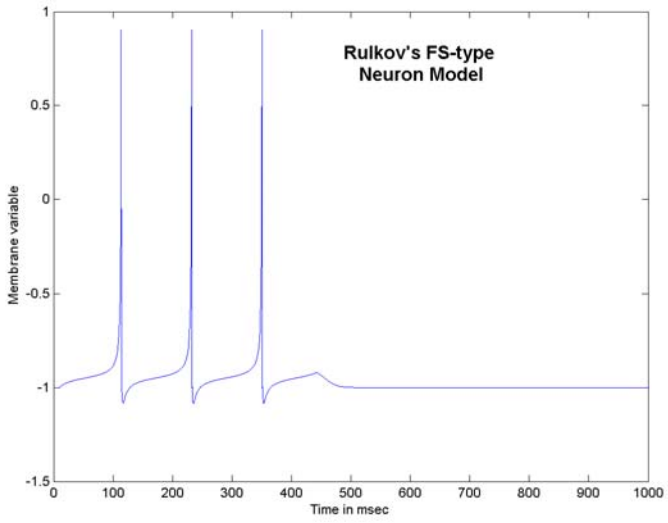


**Figure 6.9:** Response of the Rulkov FS-type neuron using the parameters given in the text. The external stimulus was applied at $t$ = 10 ms and turned off at $t$ = 440 ms.

## § 6. Calibrating an Abstract Neuron Model

Phenomenological NLD-based models such as Rulkov's or Izhikevich's are used in network simulations in order to capture the effects on network dynamics of the complex firing patterns that can be produced by the different neuron signaling types thought to be present in the population of biological neurons being modeled. Indeed, there is very little point in going to the trouble of putting together such a model if it is not presumed that these dynamics are fundamentally important to network function.

However, abstract neuron models such as the Rulkov or the Izhikevich schemata produce have no mechanistic tie to underlying biological neuron dynamics. Merely because such a model produces a realistic-looking firing response to an external stimulus with a given set of parameters at a particular level of applied stimulus, this does not guarantee that the model's responses will be equally realistic for other levels of input stimulus or for other patterns of stimulus produced by different patterns of synaptic input stimuli. An abstract neuron model that presents realistic-looking responses for only one or a few different input cases is a model that is not very useful for neural network simulation. Indeed, the use of such a model poses a serious risk that the researcher using it may "learn something that isn't true" of the biological network he wishes to study. For this reason, it is essential that one ***calibrate*** an abstract neuron model before employing it in a research study.

To calibrate a neuron model means to adjust its parameter set such that the model produces responses to different stimulus conditions that match those of its desired biological counterpart. If

necessary, one must modify the model to either produce some desired response characteristic not exhibited or to suppress some undesired response characteristic it does exhibit. Measuring a neuron's response to an applied current pulse stimulus is an important laboratory method for investigating the physiology of the neuron, but neurons in their normal biological environment are not subjected to this type of stimulus. Natural stimuli consist of different patterns of post-synaptic current produced by vectors of action potential afferent signals, both synchronous and asynchronous, with different incoming firing rates, different relative times of arrival at its different synapses, and different arrival times relative to the target neuron's own firing history.

For example, map-based models typically do not have either an absolute or a relative refractory period of any significance after firing an action potential. The refractory period of a neuron is thought to be an important factor in determining the neuron's selectivity to afferent firing rates, acting as a kind of low-pass filter to the signals it receives. To a large degree the modeler depends on the firing rate characteristics of the model in response to different test stimulus amplitudes to adequately mimic this property in a network setting. However, it should be kept in mind that the model is not explicitly designed to produce a particular refractory period characteristic, and so one is depending on refractory-like behavior to be an emergent property of the model. The only way to be sure the model actually exhibits the desired refractory-like response to realistic AP stimuli within a network is to test for it.

For example, the Rulkov neuron's response to external stimulus is determined by two terms in the model, namely

$$\beta^e \cdot I_n^{syn} \text{ and } \mu \cdot \left(\sigma + s^e \cdot I_n^{syn}\right).$$

These factors interact in determining the model's firing rate in response to pulse test stimuli, and its accommodation and burst-vs.-tonic response properties for this stimulus. When $I_n^{syn}$ is held at a constant value, both terms are merely constants and there is a multiplicity of different parameter combinations for $\beta^e$, $\mu$, $\sigma$, and $s^e$ that will produce the same firing response. To calibrate the response of the model, it is necessary to use several different stimulus levels, $I_n^{syn}$, to determine the overall set of parameters needed to produce the desired dynamical properties. Even then, it might be that the resulting model still does not adequately capture a biologically-realistic refractory time property over the range of *network* stimulus conditions possible. (It is not always necessary that the neuron model accurately capture the true refractory characteristic; it is only necessary that it capture it well enough for the network operation to behave properly). The only practical way to know this is to test for it. Then, if one finds the refractory response to be

unsatisfactory, one can modify the base model. For example, one might modify the input parameter $s^e$ to include a refractory effect. One possible way this might be done is to make $s^e$ a dynamic variable, e.g.

$$\begin{aligned} q_{n+1} &= \rho \cdot q_n + z_n \\ s_n^e &= s_{ss}^e \cdot (1 - q_n) \end{aligned} .$$

Here $q_n$ is an auxiliary variable modeling the refractory state and $z_n$ is the AP output variable for the neuron. $\rho$ is a constant, $0 \le \rho < 1$, setting the time constant of the refractory period, and $s_{ss}^e$ is the steady-state value, corresponding to the $s^e$ term in the base Rulkov model. Addition of this term will generally require re-testing and possibly re-fitting of the other model parameters.

The reference standard against which an abstract neuron model is to be compared is a physiological model, generally a Hodgkin-Huxley model of the biological neuron. In some cases an abstract model with a reasonably strong connection to physiology, such as Wilson's models, might be used in place of a full-blown Hodgkin-Huxley model, although here the limitations of Wilson's models (e.g. no post-inhibitory rebound, dubious refractory period characteristics) must be kept in mind by the modeler. In the case of the Rulkov et al. network simulations [RULK1], the calibration standard was the Hodgkin-Huxley-like neuron model of Mainen and Sejnowski [MAIN], which is a physiologically-based two-compartment H-H-like model.

The objective of calibrating the model neuron to a physiological counterpart is to provide a link between the *mechanistic* properties of biological neurons and the *functional* properties of the abstract neuron model insofar as these mechanistic properties are manifested in network behavior. Typically this means the basis of comparison will include a small network (a "netlet") of physiological neuron models rather than merely an individual physiological neuron model. The purpose of using network-based comparisons along with individual neuron comparisons is to ascertain that *network* properties are adequately accounted for in the abstract neuron model.

For example, Rulkov et al. tested their network model [RULK1] against networks of 128 and 640 Hodgkin-Huxley neuron models to ascertain that network activity waves (that is, propagation patterns of action potentials through the network) were properly captured by their models. One can see from this example that the process of calibrating abstract neuron models may entail considerable time and effort. However, without such an effort the neural network theorist will find it very difficult to convince his colleagues in neurobiology that his results are anything more than simply an exercise in mathematics. Using [RULK1] once more as an example, Rulkov et al. documented an interesting activity wave propagation effect that only emerged when their abstract neuron network model was large (25,600 RS-neurons and 65,536 RS-neurons) and did not appear

in networks comprised of "only" 6400 RS-neurons. This result can command serious merit from the neuroscience community only because Rulkov et al. were also able to demonstrate other network properties of the model that were consistent with the Hodgkin-Huxley network. In one case, their model showed an unexpected effect, which was subsequently found in the H-H network when they looked for it there. This is an example of ***predictive power*** in a functional model.

## Exercises

1. Figure 6.9 illustrates the membrane response of Rulkov's FS-type neuron model. To what subclass of FS-type neurons does the physiological neuron upon which Rulkov's model is based likely belong?
2. Show that the scaling factor needed to produce equivalence between the Wilson model and a neuron's physiological values for conductances and stimulus currents is $C/C_{act}$ where $C$ is the Wilson value and $C_{act}$ is the physiological value for membrane capacitance.
3. Derive the difference equations for simulation time step $\Delta t$ for the Wilson model equations (6.1), (6.3)-(6.5).
4. Write a computer simulation program for the Wilson model response to an injected test stimulus pulse $I_s$. Compare the results of your simulations against figures 6.1 through 6.4 for the case of $I_s$ = 0.8 applied from $t$ = 10 ms to $t$ = 190 ms. Use $\Delta t$ = 0.01 ms for these simulations.
5. Derive the difference equations for simulation time step $\Delta t$ for the Izhikevich model equations (6.6).
6. Write a computer simulation program for the Izhikevich model response to a constant step stimulus. Simulate the responses of the six Izhikevich neuron models for a test stimulus $I$ = 10 applied from $t$ = 10 ms to $t$ = 190 ms. Use $\Delta t$ = 0.01 ms for these simulations.
7. Write a computer simulation program for the Rulkov model response to a constant step stimulus. Simulate the responses of the Rulkov models for parameter and stimulus values given in Table IV. Compare your results to those of figure 6.8.
8. Write a computer simulation program for the Rulkov FS model response to a constant step stimulus. Simulate the response for parameter and stimulus values given in the text. Compare your result to that of figure 6.9.
9. Derive equations (6.16).